

N73-28323

Paper 11

ATMOSPHERIC EFFECTS IN ERTS-1 DATA, AND ADVANCED INFORMATION EXTRACTION TECHNIQUES

William A. Malila, Richard F. Nalepka, *Environmental Research Institute of Michigan (ERIM)*, Ann Arbor, Michigan*

ABSTRACT

Atmospheric effects in satellite multispectral scanner data can influence results obtained with either manual image interpretation or computer information extraction techniques. The atmosphere attenuates radiation arriving from the surface and adds an extraneous path radiance component. Initial results of an investigation of atmospheric effects in ERTS data are presented. Empirical analyses of ERTS MSS data and simultaneous airborne MSS underflight data for one frame, along with theoretical calculations of atmospheric effects, are discussed.

The effect of limited spatial resolution on the accuracy of information extracted from ERTS data also is important. Problems occur when individual resolution elements contain two or more materials. Results from an initial application of ERIM techniques for estimating proportions of materials within individual elements are presented and discussed. Very accurate determination of surface areas of small lakes is achieved.

INTRODUCTION

This paper addresses two problems that are common to all users of ERTS-1 data, namely (1) effects of the atmosphere and (2) the relatively coarse spatial resolution of the ERTS MSS. The reported work in the first area deals with understanding and verification of atmospheric effects in ERTS-1 data while, in the second, it is on an initial application to ERTS data of ERIM processing techniques designed to estimate proportions of unresolved objects in individual resolution elements. The work is part of ERTS investigation MMC-136, entitled, Image Enhancement and Advanced Information Extraction Techniques.

ATMOSPHERIC EFFECTS

By now, all ERTS investigators must be aware of the strong influence of the atmosphere on ERTS data. For example, the lesser contrasts in ERTS Band 4 images, as compared to those in ERTS Band 5,

*Formerly Willow Run Laboratories of The University of Michigan

1097

Original photography may be purchased from:
EROS Data Center
10th and Dakota Avenue
Sioux Falls, SD 57198

are in part due to the greater influence of the atmosphere in the shorter wavelength channel. Differences in atmospheric conditions within a given frame or between frames can change the spectrum of received radiances, thereby hampering image-interpretation efforts and degrading recognition processing and other information extraction with computers.

The major components of the radiance, L , received by a scanner are shown in the following simplified equation: $L = \frac{\rho}{\pi} ET + L_p$ where ρ is the diffuse target reflectance, E is the total (direct plus diffuse) solar irradiance on the target, T is the transmittance of the atmosphere, and L_p is the path radiance (i.e., extraneous radiation that does not emanate directly from the surface element under observation). All these quantities depend on wavelength, viewing and irradiation geometries, and atmospheric state. Both theoretical calculations and empirical studies with ERTS and underflight aircraft data have been carried out in a preliminary fashion for one ERTS frame (1033-15580, 25 Aug 72).

Theoretical Calculations

A radiative transfer model developed by Dr. R.E. Turner of ERIM* was used to compute the magnitude of atmospheric effects for a variety of conditions and to predict variations that depend on several different parameters. Fig. 1 illustrates the dependence of spectral path radiance on wavelength for a relatively clear condition (ground visual range, $V = 24$ km) and for a hazy condition ($V = 6.4$ km). Three observations can be made: (1) the amount of path radiance clearly increases as one approaches shorter wavelengths, (2) there is a strong dependence of path radiance on the albedo of the background surrounding the target, and (3) the path radiance is greater for the low-visibility case.

Nadir scan angle is another observation parameter. Large "scan-angle effects" often have been observed in airborne MSS data, where scan angles much larger than the $+6^\circ$ of ERTS are employed. These effects have both atmospheric and surface bidirectional reflectance causes. One would not necessarily expect to find them of significance in ERTS data, but Fig. 2 presents computed total radiance variations, for the atmosphere alone, that are as much as 8% of the minimum value for an 8% diffuse reflector observed through a clear atmosphere at $0.55 \mu\text{m}$. Percentage variations in path radiance are even greater for the background albedoes shown. The scan-angle variations are reduced for longer wavelengths and, here, are negligible at $0.95 \mu\text{m}$.

*"Importance of Atmospheric Scattering in Remote Sensing", by R. Turner, W. Malila, & R. Nalepka, Proc. of 7th Internat'l Symp. on Remote Sensing of Envir., Willow Run Labs, The Univ. of Mich., Ann Arbor, 1971.

There is, however, still an appreciable amount of path radiance at $0.95 \mu\text{m}$, as shown in Fig. 3 for a 32% reflector. This figure illustrates directly the dependence of the total and path radiances on visual range (visual range is used as a convenient method for identifying standard atmospheric aerosol profiles used in the calculations, more exact profiles can be used, if known). Note that here the total radiance received from the target in a dark background decreases with increasing haze (shorter V) while it increases for a bright one.

Fig. 4 presents the combined effects of scan angle and visual range on spectral radiances at $0.55 \mu\text{m}$ for 8% target and background reflectances. The increase of scan angle effects for lower visual ranges is clearly shown, and path radiance is a large fraction of the total.

Empirical Studies

The ERIM multispectral scanner was flown on a series of multi-altitude passes in synchronism with the ERTS-1 pass on Aug. 25th. Reflectance panels were placed on the flight line. Airborne signals from large fields, resolvable in ERTS data, were compared to signals from the reflectance panels and equivalent reflectance values were assigned to these fields, called secondary standards. Average values then were extracted from ERTS data for each of the secondary standards then converted to radiances. (The maximum radiance values listed in Table G.2-2, pg. G-14, of the ERTS Data Users Handbook were assigned to tape levels 127, 127, 127, and 63 for ERTS Bands 4, 5, 6, and 7, respectively.)

Figs. 5-8 present plots of ERTS radiance versus target reflectance for the four ERTS bands. The dashed lines are least-squares fits to the values obtained for the secondary standards. Also on the figures are trios of lines that represent approximate calculations made with the radiative transfer model for different background albedoes.

The slopes of the theoretical lines and the empirical fits agree well, but the magnitudes differ in Bands 4 and 5 for reasonable background albedoes, especially for Band 4. The reason(s) for these differences is not known at this time, but there are several possibilities: (1) The theoretical radiance values were obtained by merely multiplying band-center spectral radiances by factors of 0.1, 0.1, 0.1, and 0.3 to approximate the ERTS spectral bandwidths; more complete and accurate calculations are desirable. (2) The reflectances assigned to the secondary standards for the empirical plots appear to be too low; higher values would improve agreement. (3) The model might be in error, although checks elsewhere of sky radiance predictions have shown good agreement with measurements and with exact calculations for a pure Rayleigh atmosphere. (4) The atmospheric profile used in the calculations might not accurately represent the true condition at the test site. (5) It is possible that the ERTS calibrations are biased or we

have misinterpreted the calibration procedures. Further study of this problem is required but, nevertheless, the strong influence of the atmosphere on ERTS data has been shown.

PROPORTION ESTIMATION

A second aspect of ERTS investigation MMC-136 is testing the applicability of advanced information extraction techniques to ERTS-1 MSS data. (These techniques have been developed at ERIM with funding provided by the Supporting Research and Technology program of NASA-JSC.) One technique addresses problems associated with accurately determining areas covered by features in the scene using scanners with limited spatial resolution, like ERTS-1 MSS. Clearly, there is a serious problem for features smaller than the instantaneous field of view of the scanner. In addition, problems exist even for larger features since many of the ERTS MSS pixels overlap the boundaries between these and adjoining features. As a result, the radiation represented in those pixels is a mixture of radiation reflected from two or more materials. Since the signals generated in such pixels are not characteristic of any one material, the pixels will generally be improperly classified. Therefore, the area assigned to each material class could seriously be in error. For example, at least 25% of the pixels covering a square field of 50 acres (20 hectares) will overlap its boundaries.

At ERIM we have developed a data processing technique* to estimate the proportions of materials contained within each pixel, by taking advantage of the fact that information is gathered in several spectral bands. This permits a more accurate determination of the area covered by each material; the greater the number of spectral bands used, the more materials can be considered. We next describe and evaluate the results of an initial test of this technique on ERTS-1 MSS data.

Test Results

For this test, we selected for processing a portion of ERTS data gathered over Southwestern Michigan on Aug. 25th. A black-and-white aerial photograph of this site is shown in Fig. 9. The primary features of this site are a number of lakes and ponds of various size surrounded by trees and agricultural fields, many of them bare soil.

The goal of this experiment was to determine the surface area of the lakes and ponds. For purposes of comparison, the data were processed using a conventional recognition algorithm in addition to the proportion estimation algorithm.

*"Estimating the Proportions Within a Single Resolution Element of a Multispectral Scanner", by H. Horwitz, R. Nalepka, & J. Morgenstern, Proc. of 7th Internat'l Symp. on Remote Sensing of Environ., Willow Run Labs., The Univ. of Mich., Ann Arbor, 1971.

Initially, a number of pixels containing pure samples of each of the primary scene components (water, trees, and soil) were extracted to establish training signatures for each of these materials. The same signatures were employed by both algorithms and ERTS Bands 4, 5, and 7 were used because of problems in Band 6 data for this frame.

For the conventional recognition algorithm, each pixel was assigned to one and only one class. The resulting recognition map is shown in Fig. 10; the rejection threshold was set so that 99.9% of pixels characterized by the signatures would be recognized. Portions of eleven lakes were identified, with a total area of 451,900 m² where an area of 4503 m² (79 m x 57 m) was assigned to each pixel.

We then applied the proportion estimation algorithm to the same data set and generated the lake recognition map shown in Fig. 11. In this map, the density of each symbol is proportional to the estimated proportion of water for that pixel. It is clear on comparing this map with the aerial photo that the shapes of the lakes are more accurately reproduced. Furthermore, even small lakes and ponds are detected, for a total of 19. In addition to the map, which only illustrates ranges of proportions, the exact proportions of water in each pixel were listed. It was determined, upon examining the results, that points containing small percentages of water should be ignored to eliminate false detections. From the listing we determined that the total lake area was 965,800 m².

Finally we used the aerial photo to determine the number and actual area of the water bodies in the scene. The total area was 1,004,000 m² for 20 lakes and ponds.

In Fig. 12 we present the results for comparison. Here we see that the proportion estimation technique provided significantly more accurate results than those available using the conventional processing technique.

CONCLUSIONS

The strong influence of atmospheric effects in ERTS data has been shown. Although we have not yet directly assessed the influence of these effects, we believe that they can degrade the quality of information extracted from ERTS data. Variations in atmospheric and scene parameters, both within and between frames, will be important. Techniques for reducing the influence of these effects are being investigated.

It has been demonstrated that highly accurate area estimates can be extracted from ERTS-1 data by use of an advanced information extraction technique. For the identification of areas of lakes and ponds in the test site, the 55% error of conventional recognition techniques was reduced to 3% with proportion estimation techniques. While the magnitude of improvement shown here might not be generally achievable without further development, this technique is certain to be useful for investigations in many disciplines.

SPECTRAL DEPENDENCE OF PATH RADIANCE

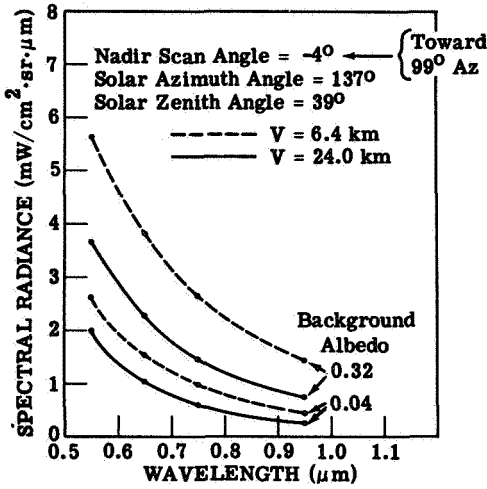


FIGURE 1

DEPENDENCE OF RADIANCE AT SATELLITE ON SCAN ANGLE, 0.55 micrometers

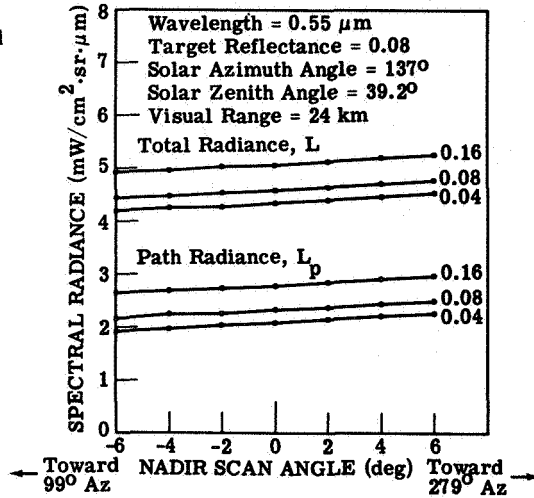


FIGURE 2

COMBINED SCAN-ANGLE AND VISUAL-RANGE EFFECTS ON RADIANCE AT SATELLITE, 0.55 micrometers

DEPENDENCE OF RADIANCE AT SATELLITE ON VISUAL RANGE, 0.95 micrometers

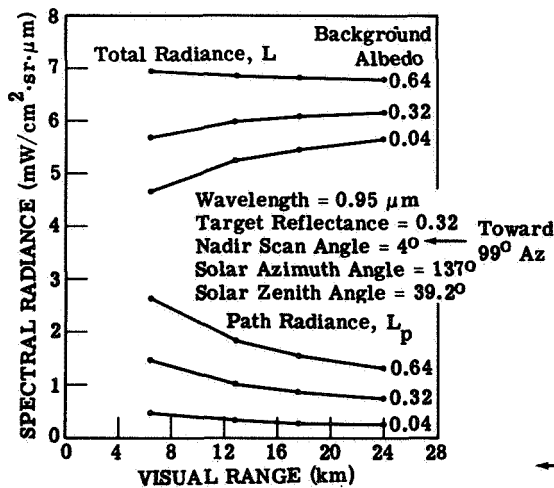


FIGURE 3

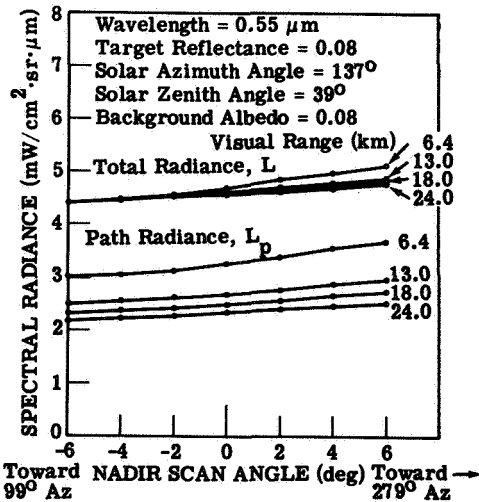


FIGURE 4



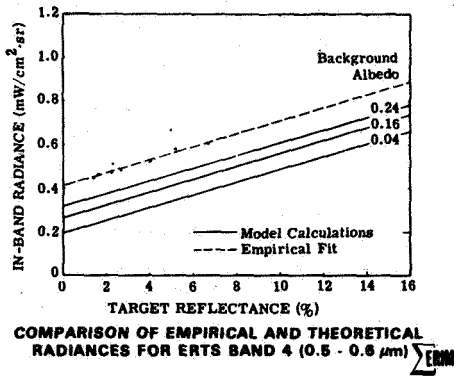


FIGURE 5

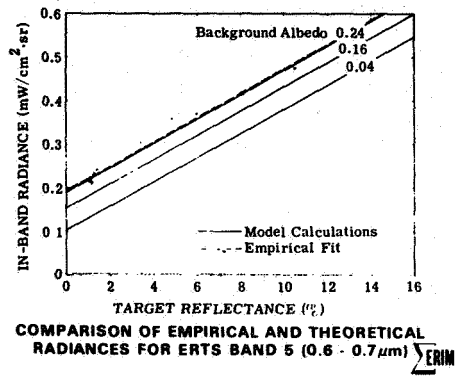


FIGURE 6

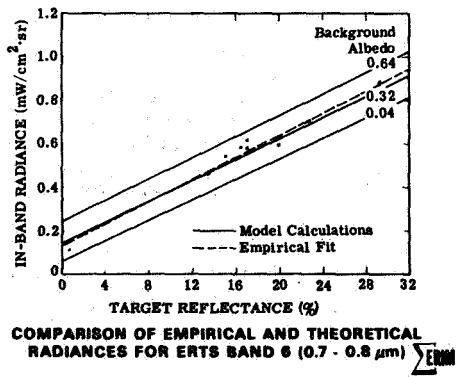


FIGURE 7

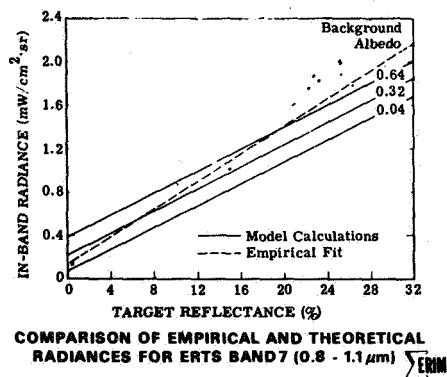


FIGURE 8

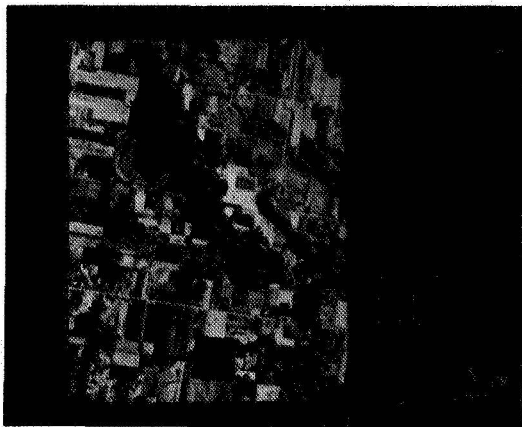
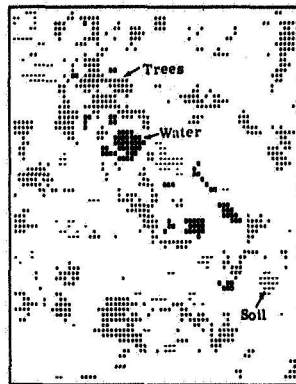


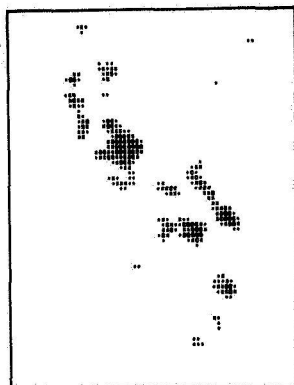
FIGURE 9



RECOGNITION
PROCESSING FOR
LAKES TEST AREA



FIGURE 10



PROPORTIONS
ESTIMATION
RESULTS FOR
LAKES TEST AREA
(Intensity of symbol
indicates proportion
of lake in each
resolution element)



FIGURE 11

COMPARISON OF PROCESSING TECHNIQUES FOR
ERTS MSS DATA FOR LAKES TEST AREA
(ERTS Bands 4, 5 and 7 Used)

	Ground Information	Recognition Processing	Proportions Estimation
Number of Lakes	20	11	19
Total Area (Meters ²)	1,004,200	451,900	985,800



Figure 12